Mesomorphic Organization and Phase Diagram of Mixtures of Polymer Terminated with Ionic Group and Oppositely Charged Surfactant

Isamu Akiba,* Yeonhwan Jeong, and Kazuo Sakurai

Faculty of Environmental Engineering, The University of Kitakyushu, 1-1 Hibikino, Wakamatsu, Kitakyushu, Fukuoka 808-0135, Japan

Received July 18, 2003; Revised Manuscript Received September 6, 2003

ABSTRACT: Mesomorphic phase behavior and phase diagram of mixtures of ω-lithium sulfonatopolystyrene (PSsul) with trimethylstearylammonium chloride (TMSAC) were investigated with differential scanning calorimetry (DSC) and small-angle X-ray scattering (SAXS). DSC measurements indicated that the PSsul and the TMSAC formed ionic aggregate with 70 wt % of PSsul and cooperatively crystallized in the aggregate. The SAXS measurements indicated the PSsul−TMSAC aggregate in solid state formed a hierarchical lamellar-*within*-lamellar structure which had two lamellae with different periodic lengths. Above melting temperature of the aggregate, the shorter period disappeared and the PSsul−TMSAC aggregate formed single lamellar structure. When weight fraction of PSsul was less than 0.7, the PSsul−TMSAC mixtures were phase-separated and had two types of mesomorphic structures attributed to TMSAC itself and the ionic PSsul−TMSAC aggregate. On the other hand, when the weight fraction of PSsul was higher than 0.7, the mesomorphic morphologies of the PSsul−TMSAC mixtures changed in order of lamellar, gyroid, and ordered sphere morphologies with increasing concentration of PSsul. The phase diagram summarizing these DSC and SAXS results was comprised of 12 regions.

1. Introduction

Polymer−surfactant mixtures and complexes have been expected to be a novel class of soft materials, such as anisotropic materials and stimuli responsive materials.[1−11] The polymer−surfactant systems spontaneously form mesomorphically ordered structure in both molten and solid states due to the attractive interactions between the polymers and the headgroups of the surfactants together with the hydrophobic interactions of the aliphatic tails of the surfactants.[1,5,7−13] Since the bonds between the polymers and the surfactants are noncovalent, the polymer−surfactant systems have various phase transitions in various length scales by slight changes of environments.[1,5,7,12] The complicated phase formations in the polymer−surfactant systems must be controlled to use the mesomorphism for functional materials. For the successful controlling of the various phase formations and transitions, detailed investigations on the phase behavior, such as phase diagrams, are of importance. For the polymer−surfactant systems that form comblike aggregates, investigations on the phase behavior have been sufficiently performed in detail in both experimental and theoretical approaches.[1,5,7,13−17]

Recently, formations of mesomorphically ordered phases of polymer blends consisting of end-functional polymers have been reported.[18−25] Since the polymers in the blends form noncovalently bonded block copolymers due to the attractive interactions between the end groups, the phase-separated structures of the blends are spontaneously organized in mesoscale just like a microphase separation of a block copolymer. These are regarded as the analogous systems of the mixtures consisting of the end-functional polymers and surfactants which have a polar headgroup and a hydrophobic tail. Since the surfactant itself forms mesomorphically organized structure, the phase behavior in the mixtures consisting of the end-functional polymer and the surfactant should be more complicated, compared with the phase behavior of the binary polymer blends consisting of the end-functional polymers. Therefore, the investigations concerned with the phase behavior of the mixtures of the end-functional polymer with the surfactant are of great interest.

In the present work, we examine to explore the complexity of the formation of mesomorphically ordered phases and to prepare phase diagrams of the mixtures consisting of polymer terminated with ionic group and oppositely charged surfactant. For these purposes, we use the mixtures of ω-lithium sulfonatopolystyrene as polymer terminated with ionic group and trimethylstearylammonium chloride as oppositely charged surfactant.

2. Experimental Section

Materials. Styrene was purchased from Wako Pure Chemicals Co., Ltd., Japan. *sec*-Butyllithium (*sec*-BuLi) of 1 mol L^{-1} hexane solution was purchased from Kanto Chemicals Co., Ltd., Japan. Trimethylstearylammonium chloride (TMSAC), 1,1-diphenylethylene (DPE), and 1,3-propane sultone were purchased from Tokyo Chemical Industry Co., Ltd., Japan.

Synthesis of ω-Lithium Sulfonatopolystyrene (PSsul). PSsul was synthesized according to the literature.[25−27] Scheme 1 shows the route of the synthesis of PSsul. Styrene was polymerized using *sec*-BuLi as initiator. The produced living polystyryllithium was end-capped with DPE and subsequently deactivated by 1,3-propane sultone. PSsul was purified by repeated precipitations in methanol. Number- and weight-average molecular weights of PSsul measured by GPC were 3.7×10^3 and 4.2×10^3, respectively. The terminal ionic group of PSsul was characterized by elemental analysis using a Yanaco CHN and S corder at the Instrumentation Center of The University of Kitakyushu. The obtained sulfur content of PSsul was 1.1%, corresponding to one SO_3^- unit in one PSsul chain.

Preparation of Mixtures. PSsul and TMSAC were weighted to desired ratio and dissolved in $CHCl_3$. The solution

* Corresponding author: phone +81-93-695-3295; Fax +81-93-695-3385; e-mail akiba@env.kitakyu-u.ac.jp.

10.1021/ma0350258 CCC: $25.00
Published on Web 10/04/2003

Scheme 1. Synthesis of PSsul

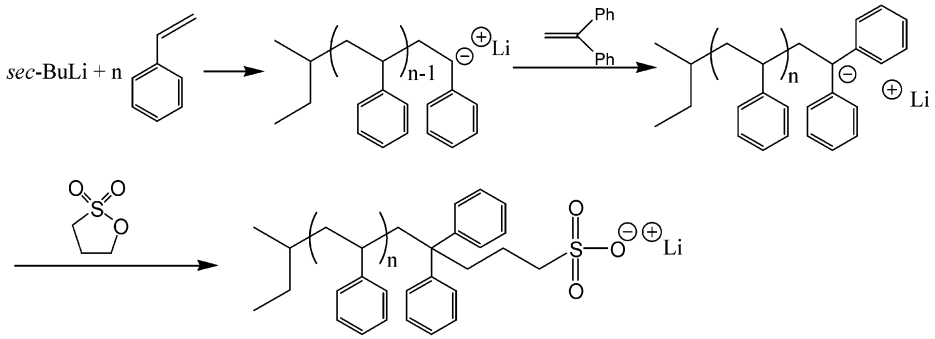

PSsul

was stirred until it became clear. After the solutes were perfectly dissolved, the solvent evaporated at 40 °C. The resulting mixtures were further dried at room temperature in reduced pressure for 1 week. The resulting mixtures were described as PSsul−TMSAC(Φ_{PSsul}), where Φ_{PSsul} denotes the weight fraction of PSsul.

Small-Angle X-ray Scattering (SAXS). SAXS measurements were performed at the BL40B2 beamline of SPring-8, Hyogo, Japan. Two-dimensional SAXS patterns were obtained by a Rigaku R-AXIS IV++ (a 30 cm × 30 cm imaging plate). The one-dimensional SAXS profiles were converted from the two-dimensional SAXS patterns by circular averaging.

Differential Scanning Calorimetry (DSC). DSC measurements were carried out using a Perkin-Elmer Pyris 1 DSC at Instrumentation Center of The University of Kitakyushu. The DSC measurements were performed at 20 deg min^{-1} of heating rate under a N_2 atmosphere.

3. Results and Discussion

Figure 1 shows DSC thermograms of PSsul−TMSAC mixtures. The thermogram of TMSAC indicates a melting peak from 80 to 90 °C. When PSsul is added to TMSAC, another melting peak appears around 60 °C. The melting peak at 60 °C becomes relatively larger with increasing PSsul contents up to $\Phi_{PSsul} = 0.7$. In the PSsul−TMSAC(0.7) mixture, the melting peak at higher temperature disappeared. Therefore, the PSsul and the TMSAC cooperatively form an ionic aggregate which includes 70 wt % PSsul (PSsul−TMSAC(0.7) aggregates), and two crystalline phases constructed with the PSsul−TMSAC(0.7) aggregates and TMSAC itself coexist in the PSsul−TMSAC($\Phi_{PSsul} < 0.7$) mixtures. On the other hand, when $\Phi_{PSsul} > 0.7$, the thermograms show a glass transition. This means that the TMSAC chains in the PSsul−TMSAC($\Phi_{PSsul} < 0.7$) mixtures cannot form crystalline packing because of the paucity of population of TMSAC. Figure 2 summarizes the melting temperatures (T_m) and glass transition temperatures (T_g) of TMSAC and the PSsul−TMSAC mixtures. Region I indicates the state coexisting two crystalline phases of the ionic PSsul−TMSAC aggregate and TMSAC itself. Region II corresponds to glassy state of the PSsul−TMSAC mixtures. Region III indicates the state coexisting liquid phase of the ionic PSsul−TMSAC aggregate and crystalline phase of TMSAC. In addition, region IV corresponds to the molten states. The SAXS experiments are examined for the PSsul−TMSAC mixtures in the characteristic four regions.

Figure 3 shows SAXS profiles for the PSsul−TMSAC($\Phi_{PSsul} \leq 0.7$) at 50 °C, corresponding to region I of Figure 2. TMSAC itself shows up to second-order

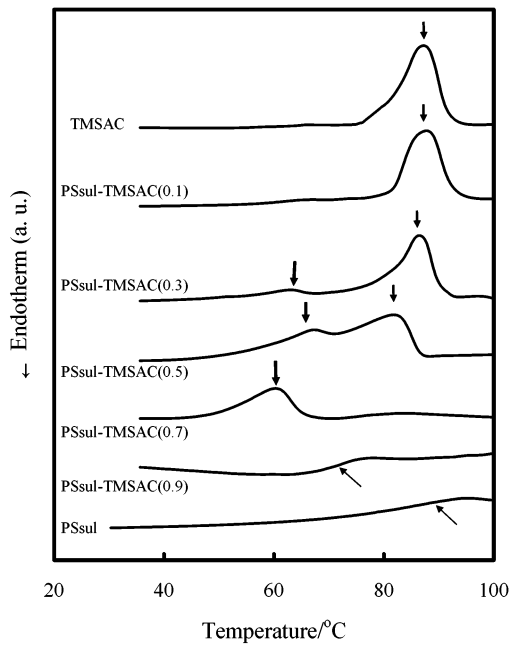

Figure 1. DSC thermograms of the PSsul−TMSAC mixtures.

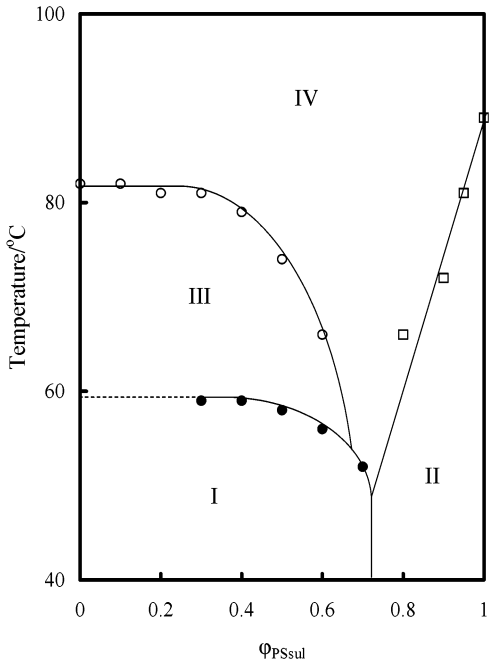

Figure 2. Plots of melting temperatures (T_m) and glass transition temperatures (T_g) of the PSsul−TMSAC mixtures against weight fraction of PSsul. Open circle, closed circle, and open square denote T_m of TMSAC, T_m of ionic PSsul−TMSAC aggregate, and T_g, respectively.

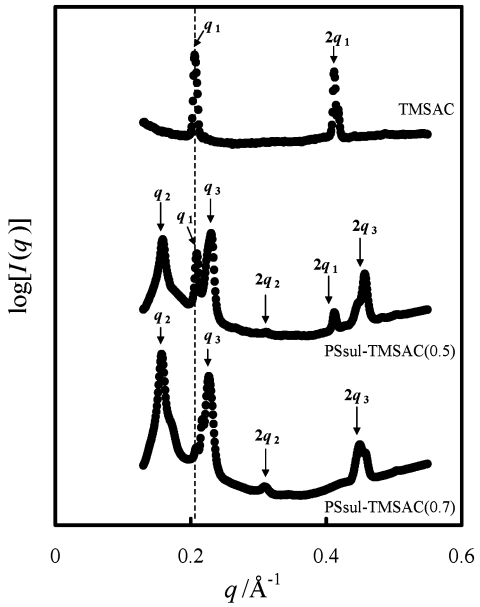

Figure 3. SAXS profiles of the PSsul−TMSAC($\Phi_{PSsul} \leq 0.7$) mixtures at 50 °C.

diffraction peaks. The q position of the first-order peak is 0.206 Å^{-1}, and the q positions are relatively assigned to 1:2. Here, q denotes the magnitude of the scattering vector defined by $q = (4\pi/\lambda) \sin(\theta/2)$, where θ is the scattering angle. Therefore, TMSAC forms the lamellar structure with 3.1 nm of the periodic length under the T_m. The periodic length of the crystalline lamellar structure is slightly longer than the chain length of TMSAC with a planar zigzag conformation (2.3 nm calculated by MOPAC) but much shorter than twice that. Therefore, it is considered that the TMSAC chains take interdigitating packing or tilted bilayer structure in which the TMSAC chains are declining to lamellar. However, if the TMSAC chains take a tilted bilayer structure, the tilting angle of the TMSAC to lamellar plane has to be ca. 42°, which is exceptionally small angle. Therefore, it is hard to consider that the TMSAC chains take a tilted bilayer structure. Thus, the TMSAC chains should take the interdigitating packing, while they may be slightly declining to the lamellar plane. On the other hand, the PSsul−TMSAC mixtures show drastically different SAXS profiles from that of TMSAC. The PSsul−TMSAC(0.5) mixture shows six diffraction peaks. Since the PSsul−TMSAC(0.5) mixture contains the crystalline phase of TMSAC itself as shown in Figure 1, the diffraction peaks at 0.206 and 0.412 Å^{-1} are attributed to the crystalline lamellar structure of TMSAC. The other peaks can be subdivided into two series. One is the peaks indicated as q_2 at 0.157 Å^{-1} and $2q_2$ at 0.313 Å^{-1} and the other q_3 at 0.230 Å^{-1} and $2q_3$ at 0.460 Å^{-1}. Since the q positions are relatively assigned to 1:2 in both series, two different lamellar structures with 4.0 nm (d_1) and 2.7 nm (d_2) of the periodic lengths coexist in the PSsul−TMSAC(0.7) mixture. d_2 is slightly longer than the chain length of TMSAC with a planar zigzag conformation, although slightly shorter than the long period of the crystalline lamellar of TMSAC itself. Therefore, the lamellar structure with d_2 period consists of crystalline aggregates of TMSAC with an interdigitating arrangement, similar to the crystalline structure of TMSAC itself. Because the PSsul−TMSAC(0.7) mixture shows a single melting peak in the DSC thermogram and does not indicate macroscopic phase separation, these lamellar structures are microscopically hybridized and behave as if one crystalline aggregate. Taking into account the results shown above, possible structures hybridized two lamellae with different periodic lengths are schematically drawn as Figure 4. If the PSsul−TMSAC(0.7) mixture takes the structure shown in Figure 4a,b, lamellar structure of the mixture should be significantly distorted or two lamellar structures with different periodic lengths should appear above T_m. However, as shown later, the PSsul−TMSAC(0.7) mixture takes a lamellar structure with a single periodic length above T_m, and it is highly ordered because the SAXS profile of the mixture indicates up to second-order diffraction. In addition, if the PSsul−TMSAC(0.7) mixture takes the structure shown in Figure 4a,b, the thickness of the PSsul layer must be equal to 1.3 nm, which is about half that of TMSAC layer. Since the weight fraction of PSsul in the mixture is 70 wt %, it is difficult for the PSsul−TMSAC(0.7) mixtures to take the structures shown in Figure 4a,b. Taking into account the composition of the PSsul−TMSAC(0.7) mixture, a structure shown in Figure 4c, the so-called lamellar-*within*-lamellar structure,[1,2,12,28] is reasonably applicable to the hybridized lamellar structure. Although the frequency of the ion−ion interaction between PSsul and TMSAC in Figure 4c is lower compared to those of Figure 4a,b, this may be left out of consideration because of much lower concentration of the lithium sulfonate group in PSsul. In addition, the periodic length of the lamellar of the TMSAC in the PSsul−TMSAC(0.7) mixture becomes slightly shorter than that of crystalline lamellar of the TMSAC itself. It is reasonable to diminish the periodic length of lamellar of TMSAC in the structure of Figure 4c because the concentration of the quaternary ammonium group at the phase boundary between PSsul and TMSAC layers is increased. On the contrary, in the other structures, it is difficult to consider more determining factors to shorten the lamellar period of the TMSAC from that of TMSAC alone. Thus, the crystalline aggregate of the PSsul−TMSAC(0.7) mixture should take the lamellar-*within*-lamellar structure as shown in Figure 4c in region I of Figure 2.

Figure 5 shows SAXS profiles for PSsul−TMSAC($\Phi_{PSsul} \geq 0.9$) mixtures at 50 °C (in region II of Figure 2). The PSsul−TMSAC(0.9) mixture shows up to fifth-order diffraction peaks. The q positions of the diffraction peaks are relatively assigned to 1:1.16:1.53:1.67:1.85. This pattern is closely corresponding to a diffraction pattern of gyroid morphology (1:1.15:1.53:1.63:1.91). Although formation of a gyroid morphology is a rare case in these polymer−surfactant mixtures, it is reasonable that the gyroid morphology is formed in the aggregates with the composition slightly deviated from that taking lamellar morphology.[29−31] In addition, PSsul−TMSAC(0.95) shows up to second-order diffraction peaks which are relatively assigned to 1:1.41. Therefore, the PSsul−TMSAC(0.95) forms ordered sphere morphology. Thus, the PSsul−TMSAC mixtures systematically change their morphology from lamellar to sphere with increasing Φ_{PSsul}, although hexagonal cylinder morphology is not observed. The characteristic features of the PSsul−TMSAC(0.9) and -(0.95) mixtures unaltered up to 70 °C ($< T_g$).

Figure 6 shows SAXS profiles of PSsul−TMSAC($\Phi_{PSsul} \leq 0.7$) mixtures. At 70 °C, the PSsul−TMSAC(0.7) mixture is in region IV and the other in

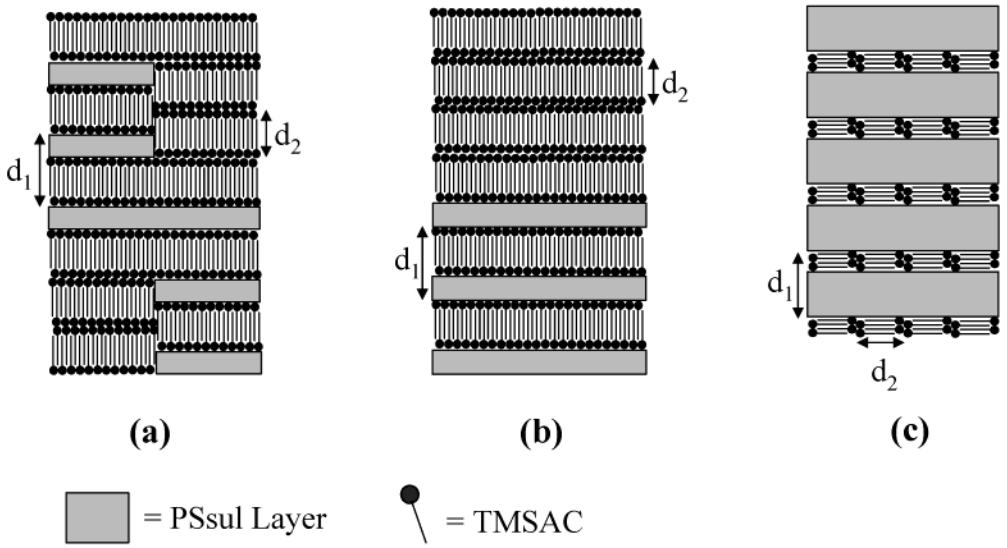

Figure 4. Schematic representations of possible structures mesoscopically hybridizing two lamellar structures with different periodic lengths. In (a) and (b), two lamellar structures are mesoscopically phase-separated. In (c), the lamellar with shorter periodic length is involved in the lamellar with longer period. This type of hybridized lamellar structure is the so-called lamellar-*within*-lamellar structure.

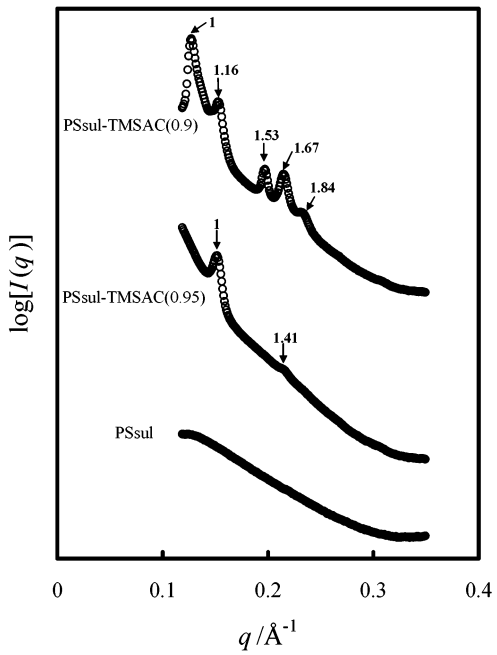

Figure 5. SAXS profiles of the PSsul−TMSAC ($\Phi_{PSsul} \geq 0.9$) mixtures at 50 °C.

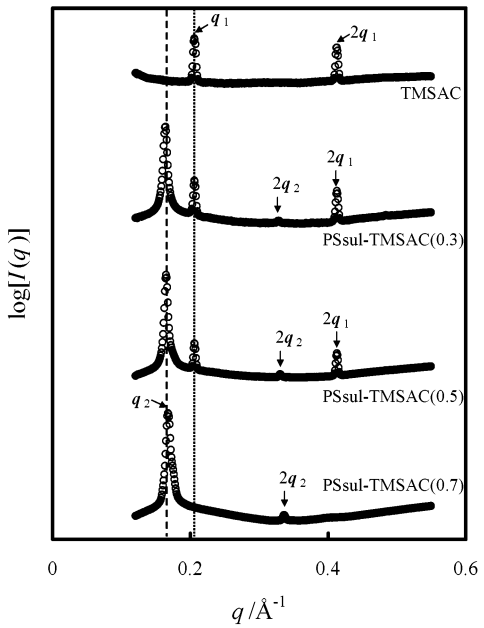

Figure 6. SAXS profiles of the PSsul−TMSAC ($\Phi_{PSsul} \leq 0.7$) mixtures at 70 °C.

region III of Figure 2. Since T_m of TMSAC is higher than 70 °C, the SAXS profile of TMSAC at 70 °C quite corresponds to that at 50 °C. On the other hand, because the PSsul−TMSAC(0.7) mixture is in the molten state at 70 °C, the SAXS profiles are changed from that of 50 °C. The SAXS profiles of the PSsul−TMSAC(0.7) mixture at 70 °C indicates a single lamellar structure with 3.8 nm of periodic length, while the lamellar-*within*-lamellar structure is formed in the PSsul−TMSAC(0.7) mixture at 50 °C. If the orientation of the TMSAC molecules in the PSsul−TMSAC(0.7) mixture is maintained above T_m, it is expected that diffraction peaks attributed to the lamellar structure of molten TMSAC are indicated. In fact, as shown later, TMSAC itself forms lamellar structure above its T_m. However, the diffraction peaks attributed to lamellar structure of molten TMSAC are not detected. Therefore, the orientations of chains of the TMSAC molecules vanished in the molten TMSAC layer of the ionic PSsul−TMSAC aggregate, and simply the lamellar structure cooperatively constructed by the PSsul and the TMSAC is maintained. PSsul−TMSAC($0 < \Phi_{PSsul} < 0.7$) mixtures show four diffraction peaks. These diffraction peaks of PSsul−TMSAC($0 < \Phi_{PSsul} < 0.7$) mixtures can be subdivided into two series. One is the peaks indicated as q_1 at 0.206 Å^{-1} and $2q_1$ at 0.412 Å^{-1} (series 1) and the other q_2 at 0.165 Å^{-1} and $2q_2$ at 0.331 Å^{-1} (series 2). Series 1 and 2 quite correspond to the diffraction peaks of the TMSAC and the PSsul−TMSAC(0.7) mixture. Therefore, in the PSsul−TMSAC($0 < \Phi_{PSsul} < 0.7$) mixtures, different two lamellar structures of TMSAC and PSsul−TMSAC(0.7) aggregate exist independently.

Figure 7 shows SAXS profiles for PSsul−TMSAC mixtures at 110 °C, which corresponds to the molten state in overall composition of the mixtures (region IV

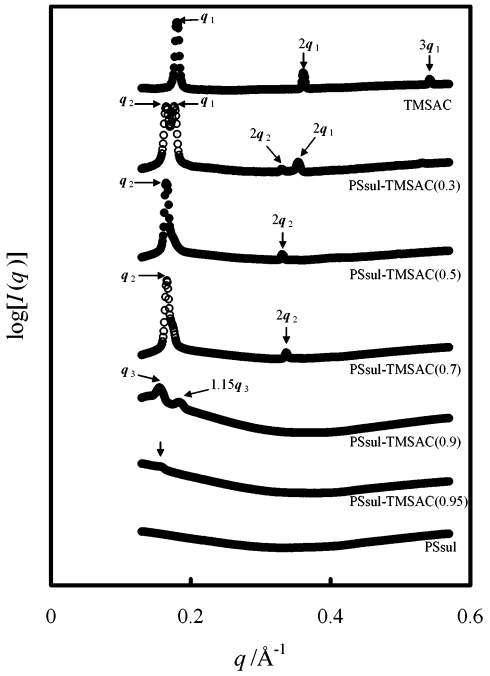

Figure 7. SAXS profiles of the PSsul−TMSAC mixtures at 110 °C.

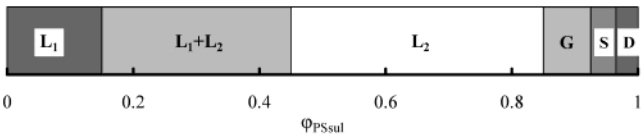

Figure 8. Relation of mesomorphically ordered structure and composition in the PSsul−TMSAC mixtures. L_1 and L_2 denote lamellar structures of TMSAC and ionic PSsul−TMSAC aggregate, respectively. G, S, and D represent gyroid, ordered sphere, and disordered morphologies, respectively.

of Figure 2). In addition, Figure 8 indicates the relation of mesomorphic structure and composition of the PSsul−TMSAC mixtures. At 110 °C, TMSAC shows up to third-order diffraction peaks which are relatively assigned to 1:2:3. Since the q position of first-order peak appears at 0.181 $Å^{-1}$, TMSAC forms a lamellar structure with 3.5 nm of periodic length in molten state. Both the PSsul−TMSAC(0.5) and -(0.7) mixtures indicate up to second-order diffraction peaks which are assigned to 1:2. Since the first-order diffraction peaks of both mixtures appear at 0.165 $Å^{-1}$, the PSsul−TMSAC(0.5) and -(0.7) mixtures form the lamellar structure with 3.8 nm of periodic length, although compositions of the mixtures are different. In addition, the periodic length of the lamellar structure corresponds to that of the PSsul−TMSAC(0.7) mixture at 70 °C. Therefore, the mesomorphically ordered lamellar structure of PSsul−TMSAC aggregate in the molten state is independent of temperature and composition. PSsul−TMSAC($0 < \Phi_{PSsul} < 0.5$) mixtures show superposed SAXS profiles of the TMSAC and the PSsul−TMSAC(0.5) mixture. Therefore, in the PSsul−TMSAC($0 < \Phi_{PSsul} < 0.5$) mixtures, different two lamellar structures of the TMSAC itself and the ionic PSsul−TMSAC aggregate exist independently at 110 °C. On the other hand, SAXS profiles of PSsul−TMSAC($\Phi_{PSsul} > 0.7$) mixtures indicate drastic changes with variation of composition. PSsul−TMSAC(0.9) mixtures show up to second-order peaks relatively assigned to 1:1.15. Although higher-order peaks indicated at 50 °C (region II of Figure 2)

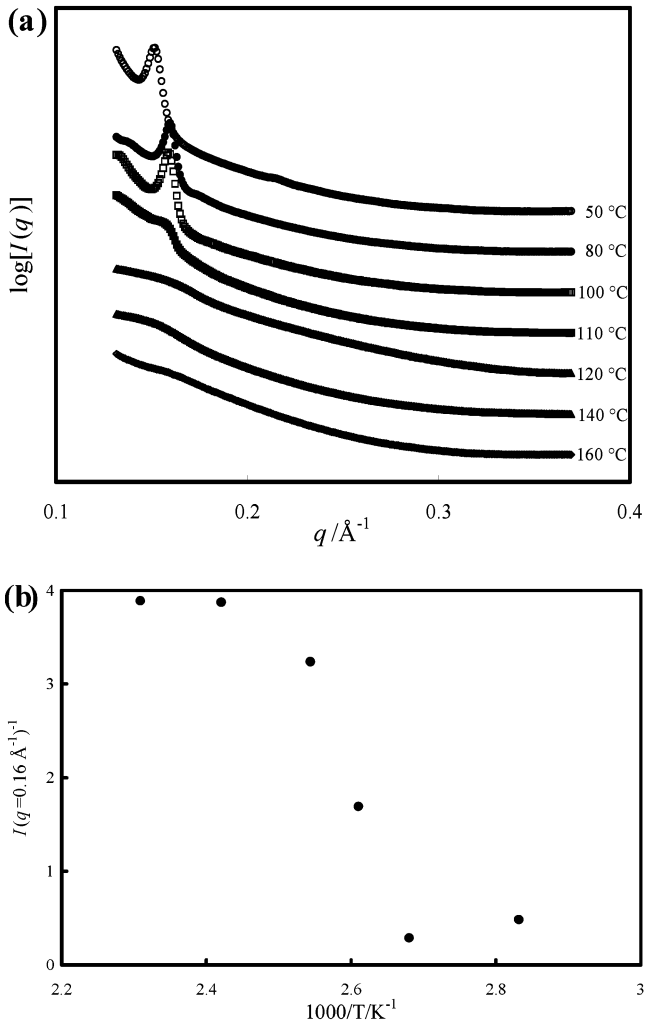

Figure 9. (a) Change of SAXS profiles of the PSsul−TMSAC(0.95) mixture with temperature. (b) Plot of the reciprocal of the intensity of the diffraction peak at $q = 0.16$ $Å^{-1}$ of the PSsul−TMSAC(0.95) mixture as a function of the reciprocal temperature.

disappeared with elevating temperature, the SAXS pattern attributed to gyroid morphology is also observed at 110 °C. In addition, the PSsul−TMSAC(0.95) mixture which forms an ordered sphere structure at 50 °C shows only one diffuse peak. Therefore, it is considered that the PSsul−TMSAC(0.95) mixture takes the ordered sphere structure containing considerable disarray at 110 °C. Then, change of the SAXS profile of the PSsul−TMSAC(0.95) mixture with temperature is investigated.

Figure 9a,b shows change of the SAXS profile and plot of the reciprocal of the intensity of the diffraction peak at $q = 0.16$ $Å^{-1}$ of the PSsul−TMSAC(0.95) mixture with changing temperature (T). A first-order diffraction peak is observed at each temperature in the range of $T < 110$ °C, although the higher-order peak disappeared above 80 °C. Hence, the PSsul−TMSAC(0.95) mixture forms ordered sphere phase below 110 °C. On the other hand, the diffraction peak is drastically weakened above 110 °C. Therefore, when $T > 110$ °C, the PSsul−TMSAC(0.95) mixture takes the disordered state. In addition, it is considered that the PSsul−TMSAC(0.95) mixture maintain the ordered sphere phase, while the structure contains considerable disarray. Figure 10 shows the SAXS profiles of the PSsul−TMSAC(0.9) mixture at 110, 140, and 160 °C. As mentioned above, the PSsul−TMSAC(0.9) mixture shows the SAXS profile attributed

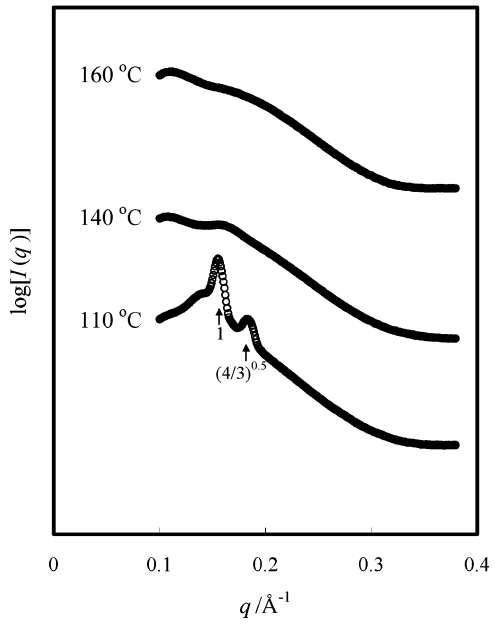

Figure 10. Change of SAXS profiles of the PSsul−TMSAC(0.9) mixture with temperature.

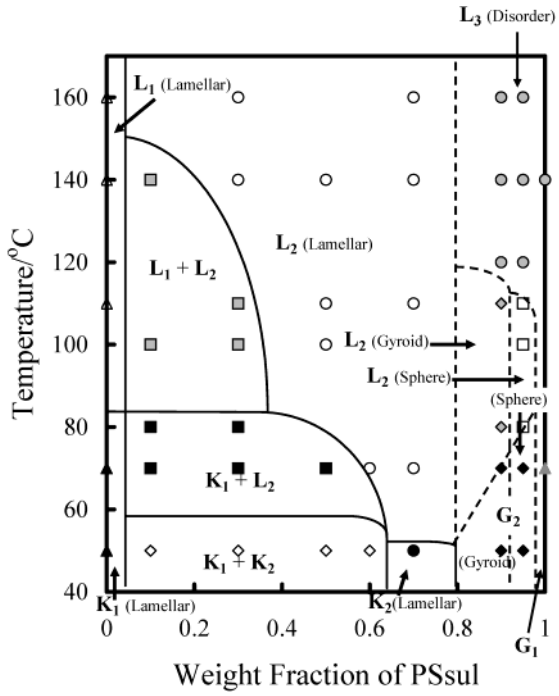

Figure 11. Phase diagram of the PSsul−TMSAC mixtures: ▲, crystalline lamellar phases of TMSAC (K_1); ●, crystalline lamellar phases of PSsul−TMSAC aggregate (K_2); ◆, glassy state of PSsul−TMSAC aggregate with gyroid or sphere orders (G_2); gray △, disordered glass state (G_1); △, liquid phase of TMSAC with lamellar order (L_1); ○, liquid phase (L_2) of PSsul−TMSAC aggregate with lamellar order; gray ◇, L_2 with gyroid order; □, L_2 with sphere order; gray ○, disordered liquid phase (L_3); ◇, $K_1 + K_2$; ■, $K_1 + L_2$; gray □, $L_1 + L_2$.

to gyroid morphology at 110 °C. On the other hand, at 140 and 160 °C, the diffraction peaks attributed to gyroid morphology disappeared, and the SAXS pattern and intensity become similar to those of the PSsul−TMSAC(0.95) mixture taking disordered phase. This feature in the SAXS profiles of the PSsul−TMSAC(0.9) mixture is already observed at 120 °C. Therefore, above 120 °C, the PSsul−TMSAC(0.9) mixture takes the disordered liquid phase.

Summarizing the results indicated above, we can draw the phase diagram of PSsul−TMSAC mixtures as Figure 11. The phase diagram of the PSsul−TMSAC mixtures is essentially divided into 12 regions. Essential characteristics are as follows. The PSsul−TMSAC(0.7) mixture forms single ionic aggregate of PSsul and TMSAC. In the ionic PSsul−TMSAC(0.7) aggregate, the PSsul and the TMSAC cooperatively form hierarchical lamellar-*within*-lamellar structure at low temperature. Since the aggregation of the PSsul and the TMSAC is maintained above T_m, the PSsul−TMSAC(0.7) mixture forms a mesomorphically ordered lamellar structure. When $\Phi_{PSsul} < 0.7$, the residual TMSAC for the PSsul−TMSAC(0.7) aggregate assembles independently and forms a crystal itself at low temperature. This phase separation is maintained up to T_m of the TMSAC. Above T_m of the TMSAC, the residual TMSAC dissolves into the TMSAC layer in the ionic PSsul−TMSAC aggregate and the PSsul−TMSAC($\Phi_{PSsul} < 0.7$) mixtures become to form a single mesomorphic lamellar structure with elevating temperature. On the other hand, when $\Phi_{PSsul} > 0.7$, the PSsul−TMSAC mixtures cannot crystallize due to the paucity of the TMSAC as a crystalline component. However, in this area, the TMSAC is not phase-separated from the PSsul due to sufficient ion−ion interaction. Therefore, when $\Phi_{PSsul} \geq 0.7$, mesomorphically ordered structures of the PSsul−TMSAC mixtures change in order of lamellar, gyroid, and sphere morphology with increasing Φ_{PSsul}.

Acknowledgment. This work is performed under the approval of the SPring-8 Advisory Committee (2003A0297-NL2-np). A part of this work is supported by funding from the Japanese Ministry of ECSST via the Kitakyushu Knowledge-based Cluster Project.

References and Notes

(1) Ruokolainen, J.; Mäkinen, R.; Torkkeli, M.; Serimaa, R.; Mäkelä, T.; ten Brinke, G.; Ikkala, O. *Science* **1998**, *280*, 557.
(2) Ruokolainen, J.; ten Brinke, G.; Ikkala, O. *Adv. Mater.* **1999**, *11*, 777.
(3) Mäki-Ontto, R.; de Moel, K.; Polushkin, E.; Alberda van Ekenstein, G.; ten Brinke, G.; Ikkala, O. *Adv. Mater.* **2002**, *14*, 357.
(4) Vikki, T.; Ruokolainen, J.; Ikkala, O.; Passiniemi, P.; Isotalo, H.; Torkkeli, M.; Serimaa, R. *Macromolecules* **1997**, *30*, 4064.
(5) Ikkala, O.; Ruokolainen, J.; ten Brinke, G.; Torkkeli, M.; Serimaa, R. *Macromolecules* **1995**, *28*, 7088.
(6) Faul, C.; Antonietti, M.; Sanderson, R.; Hentze, H.-P. *Langmuir* **2001**, *17*, 2031.
(7) Akiba, I.; Akiyama, S. *Macromolecules* **1999**, *32*, 3741.
(8) Akiba, I.; Akiyama, S. *Macromolecules* **2000**, *33*, 7967.
(9) Akiba, I.; Akiyama, S. *Mol. Cryst. Liq. Cryst.* **2000**, *339*, 209.
(10) Ponomarenko, E. A.; Tirrell, D. A.; MacKnight, W. J. *Macromolecules* **1998**, *31*, 1584.
(11) Cabane, B.; Lindell, K.; Engström, S.; Lindman, B. *Macromolecules* **1996**, *29*, 3188.
(12) Thünemann, A. F.; General, S. *Macromolecules* **2001**, *34*, 6978.
(13) Luyten, M. C.; Alberda van Ekenstein, G. O. R.; ten Brinke, G.; Ruokolainen, J.; Ikkala, O.; Torkkeli, M.; Serimaa, R. *Macromolecules* **1999**, *32*, 4404.
(14) Ruokolainen, J.; Torkkeli, M.; Serimaa, R.; Komanschek, E.; ten Brinke, G.; Ikkala, O. *Macromolecules* **1997**, *30*, 2002.
(15) Tanaka, F.; Ishida, M. *Macromolecules* **1997**, *30*, 1836.
(16) Dormidontova, E.; ten Brinke, G. *Macromolecules* **1998**, *31*, 2649.
(17) Jan Angerman, H.; ten Brinke, G. *Macromolecules* **1999**, *32*, 6813.
(18) Haraguchi, M.; Nakagawa, T.; Nose, T. *Polymer* **1995**, *36*, 2567.
(19) Haraguchi, M.; Inomata, K.; Nose, T. *Polymer* **1996**, *37*, 3611.

(20) Inomata, K.; Haraguchi, M.; Nose, T. *Polymer* **1996**, *37*, 4223.
(21) Inomata, K.; Liu, L.-Z.; Nose, T.; Chu, B. *Macromolecules* **1999**, *32*, 1554.
(22) Iwasaki, K.; Hirao, A.; Nakahama, S. *Macromolecules* **1993**, *26*, 2626.
(23) Tanaka, F.; Ishida, M.; Matsuyama, A. *Macromolecules* **1991**, *24*, 5582.
(24) Hobbie, E. K.; Han, C. C. *J. Chem. Phys.* **1996**, *105*, 738.
(25) Pispas, S.; Floudas, G.; Pakula, T.; Lieser, G.; Sakellariou, S.; Hadjichristidis, N. *Macromolecules* **2003**, *36*, 759.
(26) Quirk, R. D.; Kim, J. *Macromolecules* **1991**, *24*, 4515.
(27) Vanhoore, P.; Grandjean, G.; Jérôme, R. *Macromolecules* **1995**, *28*, 3553.
(28) Ruokolainen, J.; Saariaho, M.; Ikkala, O.; ten Brinke, G.; Thomas, E. L.; Torkkeli, M.; Serimaa, R. *Macromolecules* **1999**, *32*, 1152.
(29) Matsen, M. W.; Bates, F. S. *J. Chem. Phys.* **1997**, *106*, 2436.
(30) Lodge, T. P.; Pudil, B.; Hanley, K. J. *Macromolecules* **2002**, *35*, 4707.
(31) Alexandridis, P.; Olsson, U.; Lindman, B. *Langmuir* **1998**, *14*, 2627.

MA0350258